Bowling Green State University
ScholarWorks@BGSU

Chemistry Faculty Publications | Chemistry

12-2012

Host Guest Complexes Of Pentiptycene Receptors Display Edge-to-face Interaction

Lorenzo Mosca

Petr Koutník

Vincent M. Lynch

Grigory V. Zyryanov

Nina A. Esipenko

See next page for additional authors

Follow this and additional works at: https://scholarworks.bgsu.edu/chem_pub

Part of the Chemistry Commons

Repository Citation

Mosca, Lorenzo; Koutník, Petr; Lynch, Vincent M.; Zyryanov, Grigory V.; Esipenko, Nina A.; and Anzenbacher, Pavel Jr., "Host Guest Complexes Of Pentiptycene Receptors Display Edge-to-face Interaction" (2012). *Chemistry Faculty Publications*. 144.
https://scholarworks.bgsu.edu/chem_pub/144

This Article is brought to you for free and open access by the Chemistry at ScholarWorks@BGSU. It has been accepted for inclusion in Chemistry Faculty Publications by an authorized administrator of ScholarWorks@BGSU.

Author(s)
Lorenzo Mosca, Petr Koutník, Vincent M. Lynch, Grigory V. Zyryanov, Nina A. Esipenko, and Pavel Anzenbacher Jr.

This article is available at ScholarWorks@BGSU: https://scholarworks.bgsu.edu/chem_pub/144

CRYSTAL GROWTH & DESIGN

Article

pubs.acs.org/crystal

Host–Guest Complexes of Pentiptycene Receptors Display Edge-to-Face Interaction

Lorenzo Mosca, Petr Koutník, Vincent M. Lynch,† Grigory V. Zyryanov, Nina A. Esipenko, and Pavel Anzenbacher, Jr.*

Department of Chemistry and Center for Photochemical Sciences, Bowling Green State University, Bowling Green, Ohio, United States

Supporting Information

ABSTRACT: The pentiptycene receptors form edge-to-face complexes with a variety of aromatic guests including nitroaromatics. X-ray diffractometry revealed that compounds **1**, **2**, and **3** form host–guest assemblies with a thienyl fragment (from a neighboring molecule of **1**), benzene and nitrobenzene, respectively. X-ray studies of the three crystal structures reported here strongly suggest the edge-to-face to be a predominant binding mode between the aromatic guests and electron-rich faces of the pentiptycene aromatic cavity.

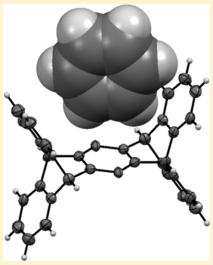

INTRODUCTION

Iptycene and pentiptycene derivatives have attracted significant attention in supramolecular chemistry in the past few decades.[1] Their appeal is largely due to their rigid framework constraining the aromatic groups between the bridgehead-carbons at an angle close to 120° as well as the presence of well-defined cavities. This results in propensity to leave voids and pores in the solid state structure. Such voids may be occupied by guest molecules that can be used to control the supramolecular architecture of the crystal, thereby providing an efficient tool for crystal engineering.

Iptycenes have been used in high-performance polymers endowed with semiconducting and luminescence properties.[2a,b] Notable examples are signal amplifying poly(phenylene ethynylene) (PPE) pentiptycene polymers by Swager, which were successfully employed as sensors for explosives, for example, in the commercial Fido sensors (Nomadics, Inc.)[2c−e]

Pentiptycene scaffolds substituted with crown ether macrocycles have been shown to bind electron-deficient aromatic molecules such as alkylviologens[3a] and cyclobis(paraquat-*p*-phenylene).[3b−d] The pentiptycene moiety provides an electron-rich cavity accommodating electron-poor guest molecules bound via π-stacking interactions, as shown by X-ray structures and ^{1}H NMR experiments.[3] An extended tweezer-like shaped pentiptycene showed affinity toward C_{60},[4a] presumably due to the favorable interaction between the electron-rich aromatic cavity and the eletron-poor polyene-like surface of the fullerene.[4b]

Recently, we reported the sensing of nitroaromatic explosives (2,4-DNT, TNT) by small-molecule, pentiptycene-based, fluorescent sensors embedded in polymer films[5] and high-surface nanofibre mats.[6] In our previous studies the synthetic protocols, efficiency of the sensing mechanism, and potential advantages for the sensing of explosives were discussed. Also, the signal transduction corresponding to an observable change of the fluorescence signal of the sensor was ascribed to photoinduced electron transfer (PET) between the high-energy excited state of the pentiptycene derivatives and the low-energy lowest unoccupied molecular orbital (LUMO) of the nitroaromatic analytes.[6] The efficiency of the PET process implies that the receptor and analyte are in close vicinity. In solution the fluorescence quenching appears to be due to simultaneous static- (PET) and collisional-quenching (nonradiative relaxation due to intermolecular collisions).[7] In the solid state (polymer matrices) the PET process increases in importance and the nitroaromatics quench the sensor fluorescence efficiently even at low analyte concentrations.[5,6]

In this study we report on the results of a structural analysis of three single crystals obtained with receptors **1**, **2**, and **3** (Figure 1) in the presence of aromatic guests. The aim of this work was to gain more detailed understanding of the interactions between iptycenes and their aromatic guests.

EXPERIMENTAL SECTION

Compounds **1**, **2**, and **3** were synthesized as previously reported[5,6] by cycloaddition of the corresponding arynes to anthracene.[8]

X-ray Experimental. Single crystals of **1** suitable for X-ray diffractometry were obtained by slow evaporation of a CH_2Cl_2 solution of **1**. Single crystals of **2**·4C_6H_6 and **3**·2$C_6H_5NO_2$ were obtained by slow evaporation of **2** in benzene and **3** in nitrobenzene. Preliminary partially refined structures showing **2**·4C_6H_6 and **3**·2$C_6H_5NO_2$ are also presented in our study focused on TNT sensing.[6] All diffraction data were acquired at 153 K on a Nonius Kappa CCD instrument using an Oxford Cryostream low temperature device. The instrument uses a graphite-monochromatized MoKα (λ =

Received: August 27, 2012
Revised: September 19, 2012
Published: September 21, 2012

 © 2012 American Chemical Society

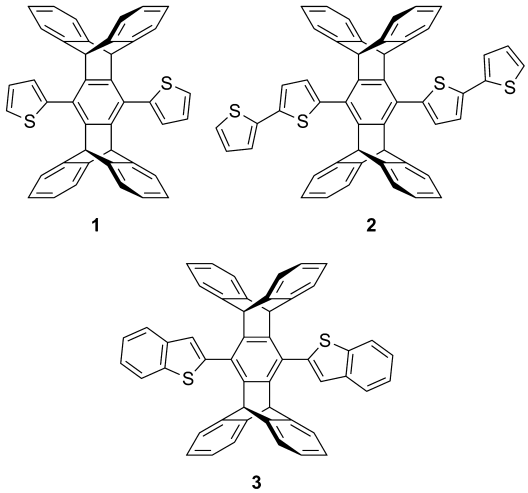

Figure 1. The structures of receptors **1**, **2**, and **3**.

0.71075 Å) wavelength. Data reduction was performed using DENZO and Scalepack.[9] The structures were solved by direct methods using SIR97[10] and refined by full-matrix least-squares on F^2[11] with anisotropic displacement parameters for all non-H atoms assigned using SHELXL-97.[12] **2**·4C_6H_6 was found to be twinned. The twin law[13] was determined using TwinRotMat[14] as found in PLATON98[14] incorporated in WinGX.[15] Details of crystal data, data collection, and structure refinement are listed in Table 1.

■ RESULTS AND DISCUSSION

Compound 1. Compound **1** (Figure 2) crystallizes in the trigonal system, and each unit cell contains nine molecules. One of the thiophene rings is disordered by rotation around the bond connecting the ring to the remainder of the molecule.[16] The crystal structure of **1** shows that the thienyl rings are almost perpendicular to the plane of the pentiptycene with a torsional angle φ = 87.9°, both thienyl rings are symmetry-equivalent through an inversion center. The aromatic rings of **1** define planes that form symmetrically equivalent angles (δ = 117.24°, ε = 121.05°, ζ = 121.71°; the planes used for this calculation are defined as the best plane that comprises the six carbon atoms pertinent to each of the benzene fragments), as shown in Figure 2 (bottom panel). Those angles deviate only slightly from the theoretical 120° and this difference may be due to the presence of an included guest.

Quite surprisingly, two molecules of **1** were found to interact in the crystal lattice. The thienyl ring of the second molecule is included into the cavity of the first pentiptycene whereby the thienyl fragment sits in the concave aromatic surface with hydrogen atoms oriented to face the π-clouds of the aromatic moieties of the pentiptycene (Figure 3). The plane of the thienyl ring is inclined at about 70° with respect to the plane of the pentiptycene. Relevant distances are shown in Table 2. It can be easily shown that the thiophene fragment established an interaction with the pentiptycene receptor and not a mere contact inclusion. The measured centroid···H distances (range: 2.658−2.751 Å) reported in Table 2 reveal the existence of interactions in the host−guest complex. Those distances are considerably shorter compared to the sum of the van der Waals radii relative to hydrogen (1.20 Å) and the extent of the benzene electron density (1.7−1.8 Å),[17] the minimum contact distance being 2.9−3.0 Å. Contacts shorter than the sum of the van der Waals radii accounts for the existence of an edge-to-face interaction.

Long-Range Features in 1. The long-range crystal structure of **1** shows interesting features. Along the c axis the

Table 1. Crystal Data and Collection Parameters

	1	2·4C_6H_6	3·2$C_6H_5NO_2$
formula	$C_{42}H_{26}S_2$	$C_{50}H_{30}S_4$·4C_6H_6	$C_{50}H_{30}S_2$·2$C_6H_5NO_2$
formula weight	591.74	1071.41	941.08
crystal system	trigonal	triclinic	triclinic
radiation type	MoKα	MoKα	MoKα
wavelength (Å)	0.71075	0.71075	0.71075
a (Å)	25.183(1)	13.3310(10)	11.9483(3)
b (Å)	25.183(1)	15.4300(10)	13.1865(3)
c (Å)	13.230(1)	15.7140(10)	17.0077(4)
α (°)	90.00	116.148(3)	110.779(1)
β (°)	90.00	89.981(3)	101.548(1)
γ (°)	120.00	91.659(2)	102.815(2)
V (Å^3)	7266.2(7)	2900.0(3)	2325.86(10)
T (K)	153(2)	153(2)	153(2)
space group	$R\bar{3}$	$P\bar{1}$	$P\bar{1}$
Z	9	2	2
μ (mm^{-1})	0.363	0.208	0.169
theta range (°)	0.998−27.49	0.973−25.00	0.984−27.49
reflns collected	3701	9938	19243
independent refl	3701	9939	10529
R_1 ($I > 2\sigma(I)$)	0.0591	0.0961	0.0566
$wR(F^2)$ ($I > 2\sigma(I)$)	0.1445	0.1741	0.1049
R_1 (all data)	0.1169	0.3355	0.1376
$wR(F^2)$ (all data)	0.1586	0.2434	0.1297
GOF on F^2	1.120	1.007	1.007
Δr_{max}, Δr_{min} /e Å^{-3}	0.299, −0.464	0.773, −0.568	0.271, −0.342
Δr (rms) /e Å^{-3}	0.059	0.109	0.056

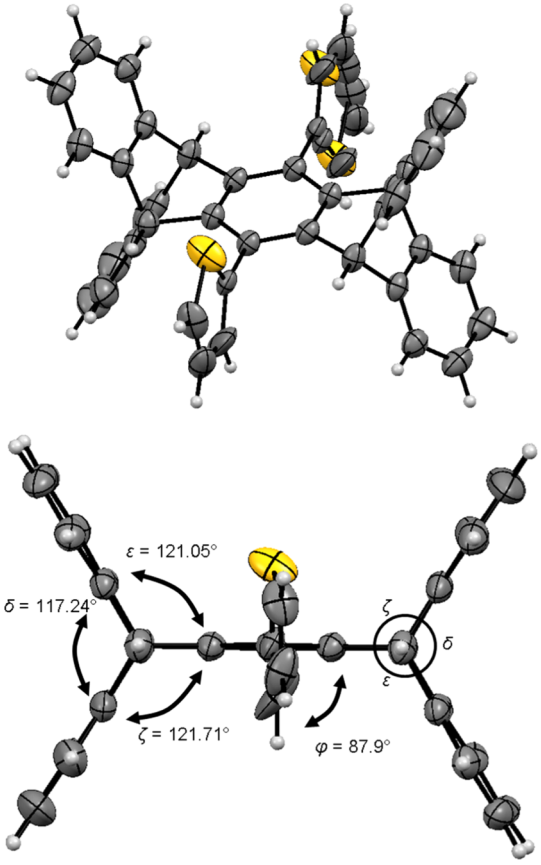

Figure 2. ORTEP representation of the structure of **1** (top panel) and lateral view (bottom panel). Angles between the thienyl unit and the central plane of **1**, as well as the angles between the aromatic planes of the pentiptycene are highlighted. Thermal ellipsoids are represented at the 50% probability level.

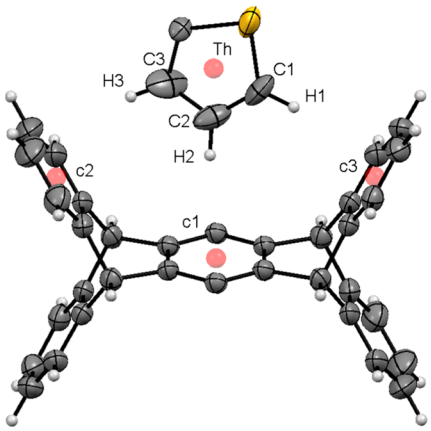

Figure 3. ORTEP representation of the structure of **1** showing the thienyl fragment included in the pentiptycene cavity. Atom labeling and centroids (red spheres) are shown to explain the distances listed in Table 2. Thienyl substituents on the host iptycene were removed for clarity. Thermal ellipsoids are represented at the 50% probability level.

crystal lattice displays a repetitive pattern of large pores formed by three different molecules of **1** arranged around the center of the pore in a triangular fashion. The length of the pore is generated by the 3-fold rotoinversion axis (Figure S4). The hollow structure thus generated has a minumum diameter of 2.0 Å (calculated from the van der Waals surface of the hydrogens located in the inner rim), which is too short to allow other molecules to be included in the pores without distorting the crystal lattice.

Table 2. Selected Distances in 1

	d [Å]
c2[a]···Th[a]	4.759
c1[a]···Th[a]	4.832
c3[a]···Th[a]	4.820
c2···H3	2.734
c1···H2	2.751
c3···H1	2.658
c2···C3	3.601
c1···C2	3.655
c3···C1	3.581

[a]c1, c2, c3 represent the centroids calculated for the aromatic rings of receptor **1**, as shown in Figure 3; Th represents the centroid calculated for the thienyl fragment.

2·4C$_6$H$_6$. Compound **2** crystallizes in the triclinic system; however, the crystal has been found to be twinned.[13] As shown in Figure 4, the terminal thiophene units are disordered by rotation about the bond forming the bithiophene moieties.[18]

The asymmetric unit contains two halves of different molecules, which reside on the inversion centers of the unit cell. The remainder of the molecules are shared between adjacent unit cells. In total, four half-molecules are present in the unit cell. Only one of the four benzene molecules interacts with the pentiptycene cavity (the **2**-to-benzene ratio is 1:4). Selected distances are reported in Table 3. The angles formed by the planes that include the thiophene rings and the plane defined by the pentiptycene receptor **2** differ from 90° (φ_1 = 74.1°, φ_2 = 178.2°). This deviation is presumably due to the higher degree of freedom of bis(thienyl) substituents, as well as to the packing of the molecules in the lattice. The angles formed between the planes of pentiptycene **2** are close to the predicted 120° value, being δ = 120.18°, ε = 121.58°, and ζ = 118.24° (angles were calculated as specified above for **1**). Those angles are symmetry-equivalent through an inversion center in the central plane of **2**. The included benzene molecule sits in the cavity with an angle of 87.59° (Figure 5); the relevant centroid···centroid and centroid···atom distances are reported in Table 3 (left columns). The distance d(c2···H6BA) = 2.865 Å is considerably shorter than the sum of the van der Waals radii of hydrogen and aromatic carbon atoms[18] suggesting a close interaction between the benzene guest and receptor **2**.

Long-Range Features in 2·4C$_6$H$_6$. The long-range lattice structure of the title compound features a repetitive pattern of alternating layers of pentiptycene molecules and benzene molecules (Figure S5). Here, the long-range features in **2**·4C$_6$H$_6$ are due to the interaction of the bithienyl unit with the aromatic cavities formed on the side of the pentiptycene. We found that the bithienyl unit in **2** is in close proximity to a second molecule of the receptor. The distances between the thienyl fragments and the aromatic cleft of the iptycene (3.35–3.48 Å) suggest the existence of a π-stacking interaction. This interaction may be responsible for the alternating layered arrangement of **2** and the benzene guests in the crystalline state. A recent example of edge-to-face and π-stacking interaction with the side-cavities of pentiptycenes was reported by Garcia-Garibay and co-workers.[19]

3·2C$_6$H$_5$NO$_2$. Compound **3** (Figure 6) crystallizes in the triclinic system. Two molecules of nitrobenzene have been

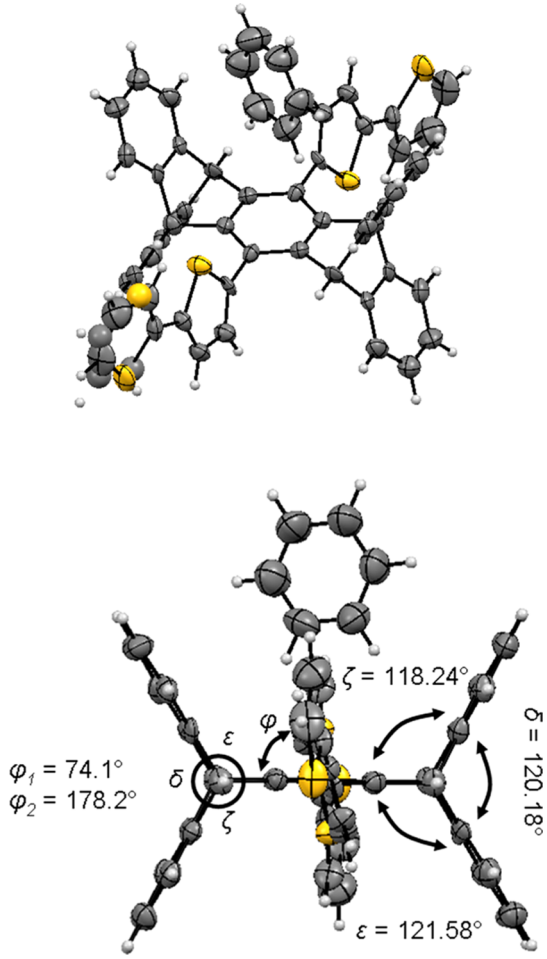

Figure 4. ORTEP representation of the structure of **2**·4C_6H_6 (top panel) and lateral view (bottom panel). Angles between the bis(thienyl) units (φ_1, pertinent to the first thiophene fragment, φ_2 for the terminal thienyl ring) and the central plane of **2**, as well as the angles between the aromatic planes of **2** are highlighted. Thermal ellipsoids are represented at the 50% probability level.

Table 3. Selected Distances for Crystals 2·4C_6H_6 and 3·2$C_6H_5NO_2$

2·4C_6H_6	d [Å]	3·2$C_6H_5NO_2$	d [Å]
c2[a]···Ph[a]	4.793	c2[a]···NB[a]	4.757
c1[a]···Ph[a]	5.094	c1[a]···NB[a]	4.804
c3[a]···Ph[a]	4.865	c3[a]···NB[a]	4.770
c2···H5BA	3.636	c2···H4BA	2.911
c2···H6BA	2.865	c2···H5BA	3.416
c1···H1BA	3.153	c1···H3BA	3.051
c1···H6BA	3.441	c1···H4BA	3.605
c3···H1BA	3.169	c3···H2BA	2.810
c3···H2BA	3.459	c3···H3BA	3.303
c2···C5B	3.998	c2···C4B	3.605
c2···C6B	3.598	c2···C5B	3.856
c1···C1B	3.908	c1···C3B	3.699
c1···C6B	4.040	c1···C4B	3.982
c3···C1B	3.803	c3···C2B	3.558
c3···C2B	3.925	c3···C3B	3.806

[a]c1, c2, c3 represent the centroids calculated for the three aromatic ring-fragments of the pentiptycene receptors **2** and **3**; Ph and NB represent the centroids calculated for the benzene guest and the nitrobenzene guest, respectively.

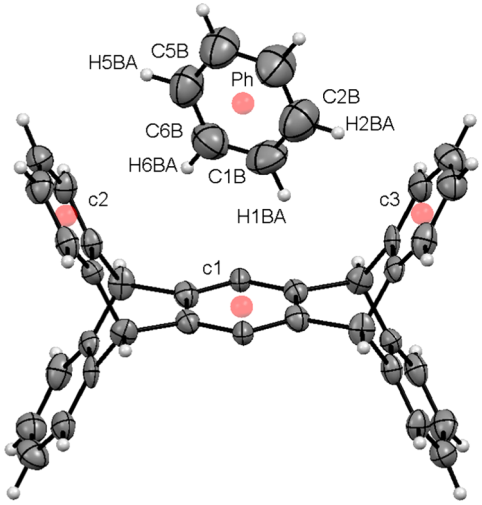

Figure 5. ORTEP representation of the structure of **2**·4C_6H_6, showing only one of the included benzene molecules. Atom labeling and centroids (red spheres) are shown for the relevant distances listed in Table 3. The two bis(thienyl) substituents on the iptycene host were removed for clarity. Thermal ellipsoids are represented at the 50% probability level.

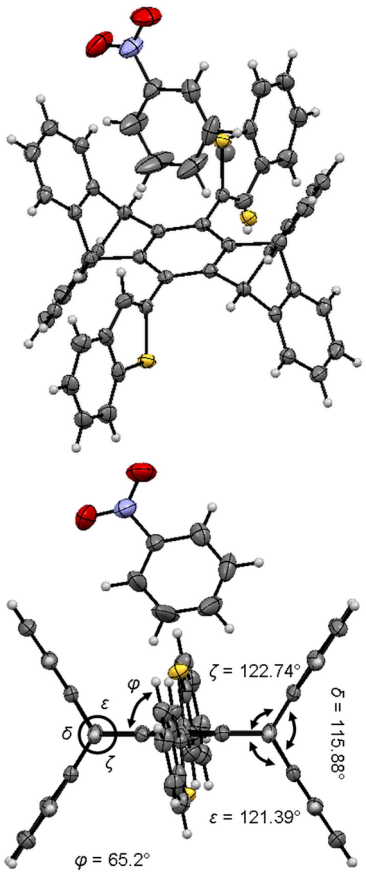

Figure 6. ORTEP representation of the structure of **3**·2$C_6H_5NO_2$ (top panel) and lateral view (bottom panel). Angles between the benzothiophene unit and the central plane of **3**, as well as the angles between the aromatic planes of the pentiptycene are highlighted. Thermal ellipsoids are represented at the 50% probability level.

found in the unit cell per each molecule of the pentiptycene. There are two half-molecules of **3** in the asymmetric unit. Both

fragments reside around the crystallographic inversion centers, and the remainder of the molecules are shared between the adjacent cells. A total of four half-molecules are present in the unit cell. Both benzothiophene moieties are disordered in such a way that the sulfur atom appears on both sides of the benzothiophene fragments.[20]

Two nitrobenzene molecules are present in the unit cell per each molecule of the pentiptycene (**3**-to-nitrobenzene ratio is 1:2). Only one of the two nitrobenzene molecules interacts with the electron-rich cavity. Relevant distances are reported in Table 3.

The angle formed by the central plane of the pentiptycene **3** and the benzothiophene fragments is $\varphi = 86.1°$ (see Figure 6). The angles defined by the aromatic planes of **3** that constitute the iptycene moiety are $\delta = 115.88°$, $\varepsilon = 121.39°$, and $\zeta = 122.74°$ (the angles were calculated by using the best planes that fits the six carbon atoms pertinent to each of the benzene fragments) and are symmetrically equivalent through the crystallographic inversion center. Figure 6 shows that the δ-angle between the two planes defined by the aromatic rings of the pentiptycene is considerably smaller than in the previous cases. This is presumably due to a stronger interaction with the electron-poor aromatic nitrobenzene. The nitrobenzene is placed in an inclined fashion inside the cavity, the angle between the nitrobenzene plane and the iptycene is 65.2°. The relevant centroid···centroid and centroid···atom distances are reported in Table 3 (right column). At least two of the measured distances, d(c3···H2BA) = 2.810 Å and d(c2···H4BA) = 2.911 Å, are shorter than the corresponding van der Waals contact distances,[18] suggesting a close interaction between the nitrobenzene guest and the pentiptycene receptor **3** (Figure 7).

■ CONCLUSIONS

In this work we present three solid state structures of pentiptycene receptors. Notably, all three structures feature an inclusion of aromatic rings in the pentiptycene cavity. In the case of **1**, a thienyl fragment of a neighboring molecule of **1** is included in the electron rich cavity of the pentiptycene. In the case of compounds **2** and **3** the guest molecules are benzene and nitrobenzene, respectively, and are also included in the pentiptycene cavity. None of the three investigated structures shows π-stacked complexes of the aromatic guest. Conversely, the maximization of the host−guest interactions is achieved through multipoint interactions between the hydrogens of the guest molecules and the π-cloud of the host molecules in an arrangement best described as an edge-to-face (or T-shaped) stacking.[21] A trend in the strength of the interaction can be drawn from the measurements of the distances between the centroids of the guest and the centroids of the iptycene aromatic rings. Thus, for example, the nitrobenzene guest molecule in **3**·$2C_6H_5NO_2$ has considerably shorter distances (0.05−0.20 Å) from the receptor walls than the benzene molecule in **2**·$4C_6H_6$. This difference could be ascribed to the different electronic nature of the two aromatic guests; the increased acidity of the hydrogens of the electron-poor nitrobenzene is likely contributing to a more stable complex as suggested by a tighter complex between **3** and the nitrobenzene. However, it is not excluded that the distances between the host and the guest may be also affected by the differences in the packing of the crystals. In **2**·$4C_6H_6$, four molecules of benzene are present per each molecule of the receptor, while in **3**·$2C_6H_5NO_2$ the host/guest ratio is 1:2. Such differences in the number of guests may translate into subtle differences in host−guest interactions.

Perhaps most importantly, this study provides a qualitative structural insight into a binding mode of aromatic species bound within the pentiptycene receptors and related materials including the pentiptycene-comprising poly[phenylene ethynylene]s,[2c,d] which were successfully employed in sensing devices for explosives.[2e] The current data support the hypothesis that the pentiptycene moiety serves as a recognition site rather just to increase porosity of the sensor materials.[2c,d] Furthermore, the structures reported here show a rather rare example of T-shaped complexes between pentiptycenes and aromatic guests[1] and provide useful insight for the design of related bowl-shaped receptor molecules and edge-to-face interactions in the field of crystal engineering and sensor development.[22]

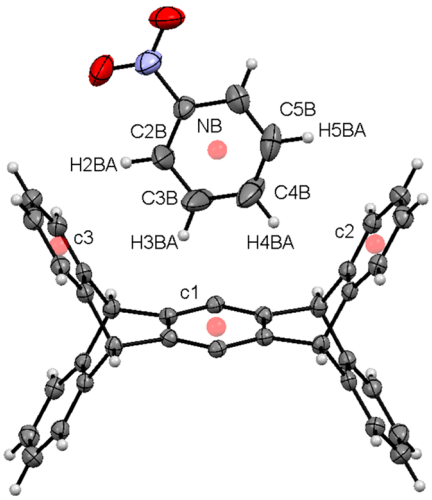

Figure 7. ORTEP representation of the structure of **3**·$2C_6H_5NO_2$, showing only one of the included nitrobenzene molecules. Atom labeling and centroids (red spheres) are shown for the relevant measurements in Table 3. The benzothienyl substituents were removed for clarity. Thermal ellipsoids are represented at the 50% probability level.

■ ASSOCIATED CONTENT

Supporting Information

Additional pictures for the crystals reported in the paper, including complete atom labeling and CIF files. This material is available free of charge via the Internet at http://pubs.acs.org.

■ AUTHOR INFORMATION

Corresponding Author

*Fax: (+) 1 419 372 9809. Tel: (+) 1 419 372 2080. E-mail: pavel@bgnet.bgsu.edu.

Present Address

†Department of Chemistry and Biochemistry, The University of Texas at Austin, Austin, TX, USA. Tel: (+) 1 512 471 4042. E-mail: vmlynch@mail.utexas.edu.

Author Contributions

The manuscript was written through contributions of all authors. All authors have given approval to the final version of the manuscript.

Funding

Financial support from Office of Naval Research (Contract No. W909MY-12-C-0031 to P.A.), AFOSR (Grant No. FA9550-05-

1-0276 273 to P.A.), the State of Ohio (WCI-PVIC), NSF (DMR-1006761 274 to P.A., EXP-LA 0731153 to P.A., CHE 0750303 to P.A.) and 275 BGSU (P.A.) is gratefully aknowledged.

Notes

The authors declare no competing financial interest.

■ REFERENCES

(1) (a) Chong, J. H.; MacLachlan, M. J. *Chem. Soc. Rev.* **2009**, *38*, 3301−3315 and literature cited herein. (b) Jiang, Y.; Chen, C.-F. *Eur. J. Org. Chem.* **2011**, *32*, 6377−6403 and literature cited herein.

(2) (a) Swager, T. M. *Acc. Chem. Res.* **2008**, *41*, 1181−1189. (b) McQuade, D. T.; Pullen, A. E.; Swager, T. M. *Chem. Rev.* **2000**, *100*, 2537−2574. (c) Yang, J.-S.; Swager, T. M. *J. Am. Chem. Soc.* **1998**, *120*, 5321−5322. (d) Yang, J.-S.; Swager, T. M. *J. Am. Chem. Soc.* **1998**, *120*, 11864−11873. (e) Cumming, C. J.; Aker, C.; Fisher, M.; Fox, M.; la Grone, M. J.; Reust, D.; Rockley, M. G.; Swager, T. M.; Towers, E.; Williams, V. *IEEE Trans. Geosci. Remote Sens.* **2001**, *39*, 1119−1128.

(3) (a) Cao, J.; Lu, H.-Y.; You, X.-J.; Zheng, Q.-Y.; Chen, C.-F. *Org. Lett.* **2009**, *11*, 4446−4449. (b) Cao, J.; Jiang, Y.; Zhao, J.-M.; Chen, C.-F. *Chem. Commun.* **2009**, *15*, 1987−1989. (c) Cao, J.; Lu, H.-Y.; Xiang, J.-F.; Chen, C.-F. *Chem. Commun.* **2010**, *46*, 3586−3588. (d) Cao, J.; Guo, J.-B.; Li, P.-F.; Chen, C.-F. *J. Org. Chem.* **2011**, *76*, 1644−1652.

(4) (a) Chong, J. H.; MacLachlan, M. J. *J. Org. Chem.* **2007**, *72*, 8683−8690. (b) Cao, J.; Zhu, X.-Z.; Chen, C.-F. *J. Org. Chem.* **2010**, *75*, 7420−7423.

(5) Zyryanov, G. V.; Palacios, M. A.; Anzenbacher, P., Jr. *Org. Lett.* **2008**, *10*, 3681−3684.

(6) Anzenbacher, P., Jr.; Mosca, L.; Palacios, M. A.; Zyryanov, G. V.; Koutník, P. *Chem.—Eur. J.* **2012**, *18*, 12712−12718.

(7) Lakowicz, J. R., Ed. *Principles of Fluorescence Spectroscopy*, 3rd ed.; Springer: New York, 2006.

(8) (a) Hart, H.; Shamouilian, S.; Takehira, Y. *J. Org. Chem.* **1981**, *46*, 4427−4432. (b) Hoffman, R. W. In *Dehydrobenzene and Cycloalkynes*; Academic Press: New York, 1967. (c) Hart, H. In *The Chemistry of Triple-Bonded Functional Groups, Supplement C2*; Patai, S., Ed.; Wiley: Chichester, 1994. (d) Cadogan, J. I. G.; Hall, J. K. A.; Sharp, J. T. *J. Chem. Soc.: C* **1967**, 1860−1862. (e) Cadogan, J. I. G.; Harger, M. J. P.; Sharp, J. T. *J. Chem. Soc.: B* **1971**, 602−607.

(9) Otwinowski, Z.; Minor., W. *Methods Enzymol.* **1997**, *276*, 307−326.

(10) Altomare, A.; Burla, M. C.; Camalli, M.; Cascarano, G. L.; Giacovazzo, C.; Guagliardi, A.; Moliterni, A. G. G.; Polidori, G.; Spagna, R. *J. Appl. Crystallogr.* **1999**, *32*, 115−119.

(11) Refinement of F^2 against all reflections. The weighted *R*-factor *wR* and goodness of fit are based on F^2, conventional *R*-factors *R* are based on *F*, with *F* set to zero for negative F^2. The threshold expression of $F^2 > 2\sigma(F^2)$ is used only for calculating *R*-factors (gt) etc. and is not relevant to the choice of reflections for refinement. *R*-factors based on F^2 are statistically about twice as large as those based on *F*, and *R*-factors based on all data will be even larger.

(12) Sheldrick, G. M. *Acta Crystallogr., Sect. A: Found. Crystallogr.* **2008**, *64*, 112−122.

(13) The twin law was (−1,0,0; 0,−1,−0.865; 0,0,1) about the 001 direct lattice direction. The twin fraction was refined to 0.456(4).

(14) (a) Spek, A. L. *PLATON, A Multipurpose Crystallographic Tool*; Utrecht University: Utrecht, The Netherlands, 1998. (b) Spek, A. L. *Acta Crystallogr., Sect. D: Biol. Crystallogr.* **2009**, *65*, 148.

(15) Farrugia, L. J. *J. Appl. Crystallogr.* **1999**, *32*, 837−838.

(16) The disorder was modelled by assigning the variable *x* to the site occupancy for the atoms of one component consisting of atoms: S1, C1, C2, C3, and C4. The factor (1−*x*) was assigned to the atoms of the alternate conformer consisting of atoms: S1a, C1a, C2a, C3a, and C4a. The geometry of the two rings were restrained to be equivalent and a common isotropic displacement parameter was refined for all atoms. In this way, the major component of the disorder, S1, C1, C2, C3, and C4, had a site occupancy factor of 80(2)%. The atoms of both rings were refined anisotropically while restraining their displacement parameters to be approximately isotropic. The displacement parameters of equivalent atoms of the rings, S1 and S1a, C1 and C1a, etc., were constrained to be equal in the final refinement model.

(17) Bondi, A. *J. Phys. Chem.* **1964**, *68*, 441−451.

(18) The disorder was modelled in the same way for both thiophene rings. The disorder was modelled by assigning the variable *x* to the site occupancy for the atoms of one component consisting of atoms: S1, C1, C2, and C3. The factor (1−*x*) was assigned to the atoms of the alternate conformer consisting of atoms: S1f, C1f, C2f, and C3f. The geometry of the two rings were restrained to be equivalent. A common isotropic displacement parameter was refined for all atoms. In this way, the major component of the disorder, S1, C1, C2, C3, and C4, had a site occupancy factor of 89(2)%. The site occupancy factor for the major component of the disordered thiophene ring on the second molecule also was found to be 89(2)%. The atoms of the major component were refined anisotropically. The atoms of the minor component had isotropic displacement parameters fixed to the values determined while determining the variable *x*.

(19) Escalante-Sánchez, E.; Rodríguez-Molina, B.; Garcia-Garibay, M. A. *J. Org. Chem.* **2012**, *77*, 7428−7434.

(20) The disorder was modelled by refining the site occupancy factors of the sulfur atom and a single carbon atom. The remaining atoms of the benzothiophene portion of the molecule appeared unaffected by the disorder. The disorder was modelled in the usual way. The site occupancy factor for S1 and C2 of the first disordered molecule was assigned the variable *x*. The site occupancy for the alternate orientation, S1a and C2c, were assigned to (1−*x*). A common isotropic displacement parameter was refined for all atoms. In this way the site occupancy factor for the major component of the disorder was refined to 91(2)%. For the second disordered molecule, the site occupancy for the major component of the disorder was refined to 62(2)%.

(21) Główka, M. L.; Martynowski, D.; Kozàowska, K. *J. Mol. Struct.* **1999**, *474*, 81−89.

(22) Hunter, C. A.; Sanders, J. K. M. *J. Am. Chem. Soc.* **1990**, *112*, 5525−5534.